AFRL-RX-WP-TP-2009-4053

TENSILE CREEP AND FATIGUE OF SYLRAMIC-iBN MELT-INFILTRATED SiC MATRIX COMPOSITES : RETAINED PROPERTIES, DAMAGE DEVELOPMENT, AND FAILURE MECHANISMS (PREPRINT)

Gregory N. Morscher, Greg Ojard, Robert Miller, Yasser Gowayed, Unni Santhosh, Jalees Ahmed, and Reji John

Pratt & Whitney

OCTOBER 2007

AIR FORCE RESEARCH LABORATORY
MATERIALS AND MANUFACTURING DIRECTORATE
WRIGHT-PATTERSON AIR FORCE BASE, OH 45433-7750
AIR FORCE MATERIEL COMMAND
UNITED STATES AIR FORCE

REPORT DOCUMENTATION PAGE

Form Approved
OMB No. 0704-0188

1. REPORT DATE *(DD-MM-YY)*	2. REPORT TYPE	3. DATES COVERED *(From - To)*
October 2007	Journal Article Preprint	

4. TITLE AND SUBTITLE

TENSILE CREEP AND FATIGUE OF SYLRAMIC-iBN Melt-INFILTRATED SiC MATRIX COMPOSITES : RETAINED PROPERTIES, DAMAGE DEVELOPMENT, AND FAILURE MECHANISMS (PREPRINT)

5a. CONTRACT NUMBER
F33615-03-D-2354-D004

5b. GRANT NUMBER

5c. PROGRAM ELEMENT NUMBER
62102F

6. AUTHOR(S)

Reji John (AFRL/RXLMN)
Greg Ojard and Robert Miller (Pratt & Whitney)
Gregory N. Morscher (Ohio Aerospace Institute)
Yasser Gowayed (Auburn University)
Unni Santhosh and Jalees Ahmed (Research Applications, Inc.)

5d. PROJECT NUMBER
4347

5e. TASK NUMBER
53

5f. WORK UNIT NUMBER
43475314

7. PERFORMING ORGANIZATION NAME(S) AND ADDRESS(ES)

Pratt & Whitney
400 Main Street
East Hartford, CT 06108-0000

Materials and Manufacturing Directorate
AFRL/RXLMN
Wright-Patterson AFB, OH

Ohio Aerospace Institute, Cleveland, OH

Auburn University, Auburn, AL

Research Applications, Inc.

8. PERFORMING ORGANIZATION REPORT NUMBER

9. SPONSORING/MONITORING AGENCY NAME(S) AND ADDRESS(ES)

Air Force Research Laboratory
Materials and Manufacturing Directorate
Wright-Patterson Air Force Base, OH 45433-7750
Air Force Materiel Command
United States Air Force

10. SPONSORING/MONITORING AGENCY ACRONYM(S)
AFRL/RXLMN

11. SPONSORING/MONITORING AGENCY REPORT NUMBER(S)
AFRL-RX-WP-TP-2009-4053

12. DISTRIBUTION/AVAILABILITY STATEMENT
Approved for public release; distribution unlimited.

13. SUPPLEMENTARY NOTES
To be submitted to Journal of American Ceramics Society
PAO Case Number and clearance date: WPAFB 07-0109, 17 October 2007.
The U.S. Government is joint author on this work and has the right to use, modify, reproduce, release, perform, display, or disclose the work.

14. ABSTRACT

The elevated temperature creep, fatigue, rupture, and retained properties of ceramic matrix composites envisioned for use in gas turbine engine applications are essential properties to understand and model for the purposes of component design and life-prediction. In order to quantify the effect of stress, time, temperature, and oxidation for a state-of-the-art composite system: the Sylramic-iBN woven fiber-reinforced, BN interphase, melt-infiltrated SiC matrix composite, a wide variety of tensile creep, dwell fatigue, and cyclic fatigue experiments were performed in air at 1204 degrees Celsius. Tests were either taken to failure or interrupted. Interrupted tests were then tested at room temperature to determine the residual mechanical properties. The retained properties of most of the composites subjected to tensile creep or fatigue was usually within 20% of the as-produced strength and 10% of the as-produced elastic modulus.

15. SUBJECT TERMS
creep, fatigue, Sylramic-iBN, SiC matrix composites

16. SECURITY CLASSIFICATION OF:			17. LIMITATION OF ABSTRACT:	18. NUMBER OF PAGES	19a. NAME OF RESPONSIBLE PERSON (Monitor)
a. REPORT	b. ABSTRACT	c. THIS PAGE			Reji John
Unclassified	Unclassified	Unclassified	SAR	36	19b. TELEPHONE NUMBER *(Include Area Code)* N/A

Standard Form 298 (Rev. 8-98)
Prescribed by ANSI Std. Z39-18

Tensile Creep and Fatigue of Sylramic-iBN Melt-Infiltrated SiC Matrix Composites: Retained Properties, Damage Development, and Failure Mechanisms

Gregory N. Morscher[2], Greg Ojard[3], Robert Miller[3]; Yasser Gowayed[4], Unni Santhosh[5], Jalees Ahmed[5], and Reji John[1]

[1] Materials and Manufacturing Directorate, Air Force Research Laboratory, AFRL/RXLMN, Wright-Patterson AFB, OH
[2] Ohio Aerospace Institute, Cleveland, OH
[3] Pratt and Whitney; East Hartford, CT
[4] Auburn University; Auburn, AL
[5] Research Applications Inc., San Diego, CA

ABSTRACT

The elevated temperature creep, fatigue, rupture, and retained properties of ceramic matrix composites envisioned for use in gas turbine engine applications are essential properties to understand and model for the purposes of component design and life-prediction. In order to quantify the effect of stress, time, temperature, and oxidation for a state-of-the-art composite system: the Sylramic-iBN woven fiber-reinforced, BN interphase, melt-infiltrated SiC matrix composite, a wide variety of tensile creep, dwell fatigue, and cyclic fatigue experiments were performed in air at 1204^{o}C. Tests were either taken to failure or interrupted. Interrupted tests were then tested at room temperature to determine the residual mechanical properties. The retained properties of most of the composites subjected to tensile creep or fatigue was usually within 20% of the as-produced strength and 10% of the as-produced elastic modulus. Also, it was observed, as in previous studies, that during creep the stresses in the matrix are relieved to some extent which results in an increased compressive stress in the matrix upon cooling and an increased stress required to form matrix cracks. Microscopy of polished sections and the fracture surfaces of specimens which failed during stressed-oxidation or after the room temperature retained property test was performed on some of the specimens in order to quantify the nature and extent of damage accumulation that occurred during the test. It was discovered that the distribution of stress-dependent matrix cracking at 1204^{o}C was similar to room temperature as-produced composites; however,

matrix cracks never appeared to propagate through thickness except for the final failure crack and matrix crack growth occurred over time at stress. Failure of the composites was due to either oxidation-induced unbridged crack growth, which dominated the higher stress regime ($\geq$ 179 MPa), whereas the lower stress regime ($\leq$ 165 MPa) was controlled by degradation of the fibers, probably caused by intrinsic creep-induced flaw growth of the fibers or internal attack of the fibers via Si diffusion through microcracks.

INTRODUCTION

Silicon carbide fiber-reinforced silicon-carbide matrix composites are currently being evaluated for aircraft engine turbine airfoil components [1-3]. Elevated temperature creep and fatigue conditions under oxidative environments are a primary concern for these types of applications. Therefore, it is essential that the effect of elevated temperature creep and fatigue conditions be well understood in order to predict useful lives for these types of composites. As part of this effort, it is critical to understand the development of damage in these materials over stress, time and environment in order to understand the mechanisms that lead to degradation in stress-strain behavior and ultimate creep or fatigue rupture.

The effect of damage development in some SiC-reinforced non-oxide reinforced has been determined for CVI SiC matrix systems with lower modulus SiC-based fiber-types (Nicalon^{TM} and Hi-Nicalon^{TM}) for creep and fatigue between 1100 and 1400^{o}C in air and argon environments [4-6]. In those composite systems, with increasing stress and time, micro cracks are formed in the 90^{o} bundles. With increasing stress and/or time, the cracks grow and extend through the CVI SiC into the load-bearing 0^{o} fiber minicomposite bundles producing through-thickness matrix cracks. Eventually a "master crack" [6] will form that becomes the site of ultimate failure. For these composite systems, fairly high strains to failure (0.5 to greater than 1%) are achieved. However, in air, times to failure are usually less than 100 hours for stresses that are in excess of the matrix cracking stress (e.g., ~ 100 MPa for the Hi-Nicalon^{TM} CVI SiC composite tested in reference 4 at 1300^{o}C).

For SiC/SiC composites reinforced with high modulus polycrystalline SiC fibers (Hi-Nicalon S) and a melt-infiltrated (MI) SiC matrix composite system a somewhat

different damage development was observed at 1315°C[7]. For the stress ranges tested (up to 172 MPa), only minor microcracking in the 90° minicomposites was observed. In some cases, these cracks were observed to extend to the surface (138 MPa) where 90° minicomposites were adjacent to the surface and into some 0° minicomposites at higher stresses (172 MPa) resulting in local fiber failure but not significant through-thickness matrix crack formation. However, for this study, creep times were usually limited to 100 hours followed by determination of retained stress-strain behavior, which was usually very high since minimal damage occurred in the composites.

It is the goal of this study to further understand the development of damage in a similar polycrystalline SiC fiber reinforced MI SiC matrix system, the Sylramic-iBN MI SiC system developed at NASA Glenn Research Center and referred to as N24A [8]. This material has undergone some of the most exhaustive testing to date of any composite system including tensile creep, 2 hour dwell fatigue, 1 hz fatigue and 30 hz fatigue at 1204°C in air for stresses ranging from 110 to 220 MPa for times up to 2000 hours in some cases [9-10]. The goal of this work is to develop life-models in general for CMC and in particular this composite system. Specimens from this wide range of tests were acquired for this study in order to determine the damage accumulation for the wide range of stress-time conditions which will be described here. Some of the specimens had been interrupted at predetermined times. For most of those specimens, a room temperature unload-reload test to failure was performed with acoustic emission (AE) monitoring in the same way as reference 7 in order to determine the remaining residual properties of the composite.

EXPERIMENTAL

The composite system evaluated is described elsewhere [8]. It consists of eight plies of 2D woven five-harness satin Sylramic-iBN, a CVI BN interphase, a CVI SiC coating to rigidize the preform and protect the fibers, slurry-infiltrated SiC particulates, and molten Si infiltrated to fill in the remaining open porosity. The five-harness fabric consisted of 7.9 tow ends per cm. The Sylramic-iBN fiber tows consist of 800 fibers approximately 10 microns in diameter. The fibers were originally produced by Dow Corning, Midland, MI but are now produced by COIC in San Diego, CA. The fibers were

subjected to a NASA-proprietary treatment in order to produce the thin (~ 100 nm) BN layer on the surface of the fiber prior to composite fabrication. The composites were fabricated at General Electric in Newark, DE. The composite volume fraction of fibers was approximately 36 to 38 %.

Some of the elevated temperature tests were performed in other studies [9-10]. All the tests performed at 1204^{o}C in lab air at SRI, Birmingham AL or CTL, Cincinnati, OH. Tensile creep tests were either performed using universal testing machines or lever-arm tensile machines. The fatigue tests were all performed in hydraulic testing machines while dwell fatigue testing was done in modified lever-arm tensile machines to control loading rates. Several fatigue loading rates were tested. Dwell fatigue (DF) consisted of a two hour hold followed by a 1 minute unload-reload back to a two hour hold. High cycle fatigue (HCF) was performed at 1 or 30 hz. All of the fatigue tests were performed for an R ratio of 0.05. Displacement was monitored using contact extensometers on the edge of the specimen, the gage section was 25 mm. The tensile specimens were approximately 155 mm long and had a contoured dogbone section where the thinnest part of the specimen in the gage section was approximately 8.2 mm. The specimen thickness was approximately 2mm. The furnace assured uniform temperature across the gage section.

For some of the specimens which were not taken to failure, a room temperature unload-reload hysteresis tensile test was performed to failure. AE sensors were placed above and below the extensometers (50 to 60 mm apart) and AE was monitored during the room temperature test using a Digital Wave Fracture Wave detector (Englewood CO) as described elsewhere [7,11]. After the test, the events were sorted as to location along the specimen length and only those events which occurred in the 25 mm gage section were used for AE analysis.

Analysis of the already crept/fatigued specimens consisted of both optical and scanning electron microscopy. Figure 1 shows a typical failed specimen. One part of the fracture surface was used for observation of the fracture surface in a field emission scanning electron microscope (FESEM – Hitachi 4700, Tokyo Japan). The other half of the specimen was cut (between 10 and 15 mm long) and polished along the edge (approximately 1mm from the exposed edge) and/or face of the specimen in order to observe and quantify the number of matrix cracks along the length. Matrix cracks caused

by time-dependent deformation had significant crack-openings and were easy to distinguish from matrix cracks formed during a room temperature retained strength tests, which were often not discernable as-polished due to crack closure from the high compressive stresses in the matrix. For the edge-polished specimens, matrix cracks were counted along the length for both surfaces (creep-formed cracks usually emanated from or to a surface) and the average value was taken as the matrix crack density.

RESULTS

All of the creep and fatigue data is shown in Figure 2. Note that open symbols indicate that the specimen did not fail and was removed for residual testing at room temperature. DF was only carried out to 250 hours and there were no failures for this condition over the entire stress range. Creep-rupture occurred at the high stresses (220 MPa) for shorter times ($\leq$ 100 hours) and for longer times (up to 2000 hours) at the lower stresses (110 and 165 MPa). Fatigue failure occurred for all of the 30 Hz HCF tests for over a wide stress range, 179 to 220 MPa, which indicates this is a more severe condition for failure compared to creep and dwell fatigue conditions. The 30 Hz HCF specimen tested for the peak stress condition of 165 MPa exceeded the run-out condition of 10^7 cycles (42,000,000 cycles survived) and was tested at room temperature for determination of residual properties. For comparison, 0.33 Hz fatigue data for the same type of composite system from Kalurri et al. [12] is plotted on Figure 2 showing similar behavior.

Residual properties of specimens that did not fail

More than twenty five different specimens were tested at room temperature after being subject to tensile creep or fatigue as well as two as-produced specimens for comparison. The stress-strain behavior and AE behavior is shown in Figure 3 for some representative specimens. The 220 MPa DF specimen was the only creep or fatigue specimen that survived the 220 MPa applied stress condition for any significant time. The degradation in ultimate strength after the 220 MPa, 168 hour, DF condition is evident.

For the specimens that had experienced creep there was an increase in the stress above which non-linearity occurs, i.e., the proportional limit stress. There was also an

increase in the stress at which significant, high energy AE occurs ("AE Onset" in Figure 3b). AE onset stress has been shown to be a good parameter for the onset of significant matrix cracking in this composite system [11]. Figure 4 shows the increase in AE matrix cracking stress (AE onset stress) with time dependent strain for some of the specimens. This can be explained by the increase in residual compressive stress in the matrix with creep or fatigue. The amount of residual compressive stress in the matrix can be determined from the intersection of the top part of the hysteresis loop with the original loading curve (Figure 3a) [13]. For as-produced specimens the residual compressive stress is about 50 MPa as was observed in reference 11. However, after tensile creep, the matrix residual compressive stress increases to over 100 MPa. Similar behavior was observed in reference 7 which was attributed to matrix relaxation during creep. Upon unloading, the matrix is in greater compression which must be overcome in order to produce and propagate matrix cracks. Figure 5 shows the effect of residual compressive stress on AE onset stress. There is nearly a direct relationship between the two. It should be noted that for the higher stress conditions, 192 and in particular 220 MPa, significant matrix cracking had occurred in the specimens tested at room temperature as will be discussed below. Therefore, the AE onset stresses for 192 and 220 MPa mask the fact that there already were some large matrix cracks formed during the elevated temperature stressed-oxidation condition. However, for specimens exposed to 165 MPa and lower stresses at elevated temperature, matrix cracking was minor (see below) and the increase in AE onset stress corresponds to the stresses required to form and propagate initial matrix cracks of significant size, i.e., the matrix cracking stress increased with low stress creep.

The ultimate properties are shown in Figure 6 for the different specimens. Note that for applied creep/fatigue stresses of 165 MPa or lower, there is very little if any degradation in ultimate strength, even for specimens subjected to nearly 250 hours. There appears to be a 10% drop in strength of specimens tested at 193 MPa up to 250 hours and about a 20% drop for specimens tested at 220 MPa for 250 hours. Specimens that survived greater than 1000 hours at lower stresses showed greater degradation in room temperature ultimate strength. The room temperature strength of the specimen that survived 1239 hours at 110 MPa was degraded about 20% compared to as-produced

material. Whereas the room temperature strength of the two specimens that survived greater than 2000 hours of creep at 110 and 165 MPa degraded almost 50% of the as-produced composite strength. It should also be noted that the retained room-temperature elastic modulus was only reduced slightly, as much as 10% after the creep or fatigue exposure [10].

Optical microscopy along the length

In order to quantify the extent of damage development in the gage section of the specimens subjected to creep and fatigue, over a dozen specimens were polished along the length (loading direction). Most specimens were aligned so that the edge was ground and polished (usually about 1 to 1.5 mm from the edge surface). A few specimens were aligned along the face of the specimen.

For edge aligned specimens, no cracks were observed for the specimens subjected to 110 MPa. For 165 MPa applied stresses and above, surface 90^o minicomposite micro cracks (Figure 7a) and inner back-to-back 90^o minicomposite cracks were evident for stress-temperature conditions up to 250 hours (Figure 8b). For 193 MPa applied stresses and above, cracks which penetrated up to two plies in from the face were common (Figure 7b). With increasing time and stress, unbridged cracks were observed along the length for 165 MPa and greater applied stress conditions (Figure 8). However, even for the specimens subjected to the highest stresses (220 MPa), these unbridged surface cracks typically extended only two plies and sometimes three into the thickness of the specimen. The presence of unbridged regions of cracks filled with a glass indicates that the fibers had failed at some significant period of time prior to ultimate failure of the composite.

In order to quantify matrix cracking, the crack density, number of cracks per mm, and the depth of cracks were recorded and are plotted in Figure 9. It is evident that with increasing stress and time that the number of cracks increases and the depth of the matrix cracks increase. However, for most cracks, even for specimens tested at 220 MPa, very few appear to propagate through the thickness of the specimen. When polished along the face of the specimen so that cracks can be observed along the 8.2 mm width, matrix cracks rarely appear to traverse the width either for the 220 MPa stress-condition experiments.

At room temperature, matrix cracks do appear to go through the cross-section of the composite at the higher stresses ($\geq$ 200 MPa) [11]. In reference 11, it was shown that the normalized cumulative AE energy was nearly directly proportional to measured matrix crack density when plotted versus stress. The matrix crack density versus stress measured in this study for elevated temperature tested specimens is compared to the room temperature data in Figure 10. Note that at the lower stresses where low energy AE events predominate and are caused by tunnel cracks which propagate through the 90^{o} minicomposites. The formation and propagation of bridged-matrix cracks at room temperature relates to the high energy AE events. If the low energy event data is removed from the AE and only the high energy event data is used, there is a very good correlation between the room temperature and elevated temperature stress-dependent matrix crack density with the exception that the elevated matrix crack density are not through-the-cross-section. The elevated temperature specimen crack densities tend to fall below the room temperature distribution. It should be noted that the method of counting cracks (taking the average of the cracks emanating from both surfaces) probably underestimates the matrix crack density. If these cracks formed and grew through-thickness at room temperature, some of the cracks would link up from both sides but others would not and go through-thickness depending on how close the matrix crack planes are to one another. Consequently, the crack density shown in Figures 9 and 10 represents the "minimum" crack density, whereas the "maximum" crack density for a given stress would be approximately twice that value. Therefore, from a modeling perspective, the room temperature derived matrix crack density is a good starting point for matrix crack density at elevated temperature as long as the depth of matrix cracks at elevated temperatures at a given stress is taken into consideration.

FESEM fracture surface examination

In order to assess the nature of failure for the composites, the actual fracture surfaces were examined using a FESEM. Note that when the specimen failed the furnace was immediately shut off so that the time at temperature that the interior of the fracture surface was exposed to significant temperatures and prolonged oxidation was only a few minutes at most. Thirteen specimens were examined from the HCF (220 MPa, 192 MPa,

179 MPa, and 165 MPa), DF (220 MPa) and creep (110 MPa and 165 MPa) specimens (Figure 2) that failed at temperature or at room temperature post creep or fatigue exposure.

For specimens subjected to stresses of 179 MPa and above, the predominant feature on the fracture surface was a large unbridged crack. In other words, regions of the fracture surface were oxidized including fiber fracture surfaces, BN region, and matrix surface as observed from the polished sections. The rest of the fracture surface was not oxidized, i.e., the SiC matrix surface, fiber fracture surface, and BN interphase were all not oxidized and fiber pullout was prevalent. At these stresses, unbridged cracks typically propagated from the edge of the cross-section (Figure 11) or from the face of the cross-section (Figure 12) always appearing to emanate from or at least include one corner of the specimen cross-section.

Again, the fact that fiber surfaces are oxidized indicates that these fibers failed before the ultimate failure event of the composite. The oxide layer that covers the fibers does appear to be thicker near the edge and is thinner away from the edge indicating that the fibers closer to the edge probably failed earlier [14]. The fact that no oxidation is observed on the opposite edge or at the surface of the specimen indicates that the matrix crack that led to ultimate failure was not through-the-cross-section.

The fracture surfaces of specimens subjected to stresses at 110 and 165 MPa either had a very small region of oxidation on the fracture surface or no real evidence of oxidation-induced embrittlement on the fracture surface. For two specimens that ruptured during creep, a triangular-shaped oxidized region of the fracture surface emanated from one corner of the fracture surface about two plies deep at the edge (the deepest part) and about 5 mm long along the width of the cross-section for the 165 MPa creep specimen which failed at 478 hours and about 2 mm long along the width of the cross-section for the 110 MPa specimen which failed at 1953 hours. Three specimens did not fail at temperature and were subsequently tested at room temperature showed no evidence of oxidation at the fracture surface: a 165 MPa 30 Hz HCF specimen that survived 42,000,000 cycles, a 110 MPa creep specimen that survived 2036 hrs (Figure 13), and a 110 MPa creep specimen that survived 1269 hours.

DISCUSSION

For this composite system, two mechanisms appear to be the cause of time-dependent strength-degradation: (1) oxidation-assisted matrix crack growth and (2) fiber degradation not associated with oxidation. These two mechanisms are complimentary; however, the former dominates the higher stress – shorter time conditions whereas the latter mechanism controls the lower stress – long time conditions.

Oxidation-Induced Unbridged Crack Growth

For higher applied stress conditions (greater than 165 MPa), non-through-thickness fiber-bridged matrix cracks that intersect the surface of the composite are exposed to the oxidizing environment. Oxygen ingress into the crack occurs, BN and SiC react to form gaseous species and solid borosilicate reaction products that fuse fibers together (similar to intermediate temperatures – see references 14 and 15). After some time fibers in the oxidized matrix cracks fail for a number of possible reasons: intrinsic fiber degradation, stressed-oxidation degradation of fibers, and/or local stress-concentrations created from local-load sharing conditions as a result of strongly bonded fibers. The result is transverse unbridged microcracks of significant depth. One, several, or many of these cracks exist along the length of the specimen depending on the stress-state (Figure 9). The number of matrix cracks along the length of the specimen is essentially the same as observed for room temperature stress-strain (except that they are non-through-thickness at 1200^{o}C). These unbridged matrix cracks result in redistribution of load to the intact region of the composite cross-section and local stress-concentrations near the crack tip. Ultimately one of these cracks becomes the source of rupture as time continues.

The nature of failure for the specimens that have significant unbridged matrix cracks existing and growing for significant times prior to failure can be compared to notched specimens. The net section stress, NSS, of the remaining pristine portion of the specimen cross section can be determined from the load applied and remaining fiber-bridged cross-sectional area. The normalized net section stress can be determined as:

$$\text{Normalized NSS} = \text{NSS}/\sigma_{ult}(T) \qquad \text{Equation 1}$$

where $\sigma_{ult}(T)$ is the fast-fracture strength of the composite. Since the times to failure for composites which exhibited significant unbridged cracks was relatively short (< 100 hours), $\sigma_{ult}(T)$ of the as-produced composites was used at the temperature where the composite was failed. For specimens that failed due to creep or fatigue at temperature, $\sigma_{ult}(1200^{o}C)$ = 377 MPa was used. For specimens that did not fail during creep or fatigue and were then tested at room temperature, $\sigma_{ult}(RT)$ = 450 MPa was used. Figure 14 shows the Normalized NSS data for some the crept and fatigued specimens of this study and compared to edge-notched [16] and face-notched data [17] for the similar MI composites. For the limited data shown here, the specimens tested under constant load (creep), DF, or 1 hz fatigue appear to follow the room temperature mild notch-sensitivity trend. However, the HCF specimens appear to be more sensitive to the size of the unbridged matrix crack.

Fiber Strength Degradation Not Due to Oxidation

At lower applied stresses, degradation in composite strength was due to a fiber-degradation mechanism not caused by oxidation. For example, the fact that the room temperature ultimate residual strength of the 110 MPa 2036 hour specimens was only slightly greater than one half the strength of the as-produced strength with no evidence for an oxidation-induced cause for failure indicates fiber degradation. Two potential mechanisms for this behavior can be considered for this type of a mechanism. Most likely, fiber degradation is due to an intrinsic creep-controlled flaw growth mechanism. Creep rupture of SiC fibers has been well documented the cause of which linked to diffusional creep mechanisms [18]. However, another possibility would be due to diffusion of free Si from the composite matrix which has been observed to attack fibers and degrade composites with no stress above 1350^{o}C [19]. This seems more unlikely because no such mechanism has been observed at temperatures lower than or equal to 1300^{o}C for the times considered here, although stress may enhance diffusion of free Si and lead to a similar effect. For example, Figure 15 shows evidence of Si diffusion into some regions of 90^{o} minicomposite microcracks and the unbridged region of a 0^{o} minicomposite crack for a specimen that ruptured after 1500 hours at 165 MPa creep.

For the two specimens discussed above which ruptured at 110 and 165 MPa after long times there was a small oxidation-induced unbridged region of the fracture surface. These cracks probably began as 90^{o} tunnel cracks which after long periods of time propagate into a few load-bearing tows and lead to a combination of the two processes where the synthesis of a small unbridged crack and the internal degradation of fibers in the bulk of the composite after long periods of time lead to rupture or significant strength degradation. It is interesting to note that the 110 MPa specimens that did not fail during creep for long times and the 165 MPa 30 hz fatigue run out specimen did not exhibit any oxidation-induced unbridged crack regions at the fracture surface or along the polished sections.

CONCLUSIONS

Excellent creep-rupture and fatigue properties were demonstrated for the Sylramic-iBN fiber-reinforced melt-infiltrated composite system. Two clear mechanisms led to elevated temperature strength degradation: (1) oxidation-induced unbridged crack growth and (2) fiber strength degradation probably due to an intrinsic creep-controlled flaw growth mechanism or internal attack of the fibers from Si diffusion. The first mechanism was dominant at higher stress conditions ($\geq$ 179 MPa) whereas the second mechanism was dominant at lower stresses ($\leq$ 165 MPa) and longer times. It was demonstrated that the damage development in this composite was the growth of matrix cracks and increasing number of matrix cracks with stress and time. The matrix crack densities were very similar to matrix crack densities measured at room temperature on as-produced specimens. Therefore, the relationships already established for stress-dependent matrix crack density [11] provides a good basis for mechanistic-based models for this material system. However, the 1204^{o}C matrix crack densities for creep and fatigue specimens did not appear to propagate through the cross-section except for the final failure crack. The unbridged cracks had the same effect as notched tensile behavior and the 30 Hz fatigue condition had a more detrimental effect on life properties compared to lower fatigue conditions and creep.

In order to further improve these composites, higher matrix cracking stresses would be required to counter oxidation-induced unbridged crack growth. This could be

achieved with fiber-architecture modifications if desired. In order to improve long-time, low stress properties, an improvement in fiber creep rupture properties would be required, which has been demonstrated for further modifications to the Syramic-iBN fiber [20].

ACKNOWLEDGMENT

The Materials & Manufacturing Directorate, Air Force Research Laboratory (AFRL/RXL), Wright-Patterson AFB sponsored this work under contracts F33615-01-C-5234 and F33615-03-D-2354-D004.

REFERENCES

1. D. Brewer, "HSR/EPM Combustor Materials Development Program," Mater. Sci. Eng. A, Vol. A261 (1999) pp. 284-291.
2. D. Brewer, G. Ojard, and M. Gibler, "Ceramic Matrix Composite Combustor Liner Rig Test," ASME Turbo Expo 2000, Munich Germany, May 8-11, 2000, ASME Paper 2000-GT-0670
3. G.S. Corman and K. Luthra, "Silicon Melt Infiltrated Ceramic Compsoites (HiPerComp^{TM}" ***Handbook of Ceramic Composites,*** Ed. N. Bansal, pp. 99-115 (Kluwer Academic; NY, NY: 2005)
4. S. Zhu, M. Mizuno, Y. Kagawa, J. Cao, Y. Nagano, and H. Kaya, "Creep and Fatigue Behavior in Hi-Nicalon^{TM}-Fiber-Reinforced Silicon Carbide Composites at High Temperatures", J. Am. Ceram. Soc., 82 [1] 117-28 (1999)
5. S. Zhu, M. Mizuno, Y. Kagawa, and Y. Mutoh, "Monotonic tension, fatigue and creep behavior of SiC-fiber-reinforced SiC-matrix composites: a review", *Comp. Sci. Tech.*, 59 833-851 (1999)
6. J. Chermant, G. Boitier, S. Darzens, G. Farizy, J. Vicens, and J.C. Sangleboeuf, "The Creep Mechanism of Ceramic Matrix Composites at Low Temperature and Stress, by a Materials Science Approach" *J. Euro. Ceram. Soc.*, 22 2443-2460 (2002)

7. G.N. Morscher and V.V. Pujar, “Creep and Stress-Strain Behavior after Creep for SiC Fiber Reinforced, Melt-Infiltrated SiC Matrix Composites,” *J. Am. Ceram. Soc.*, **89** [5] 1652-1658 (2006)
8. J.A. DiCarlo, H-M. Yun, G.N. Morscher, and R.T. Bhatt, "SiC/SiC Composites for 1200^{o}C and Above" ***Handbook of Ceramic Composites,*** Ed. N. Bansal, pp. 77-98 (Kluwer Academic; NY, NY: 2005)
9. G. Ojard, Y. Gowayed, J. Chen., U. Santhosh, J. Ahmad, R. Miller, and R. John, “Time-Dependent Response of MI SiC/SiC Composites Part I: Standard Samples”, Ceram. Eng. Sci. Proc., 2007 in print.
10. G. Ojard, A. Calomino, G. Morscher, Y. Gowayed, U. Santhosh, J. Ahmad, R. Miller, and R. John, “Post Creep/Dwell Fatigue Testing of MI SiC/SiC Composites”, Ceram. Eng. Sci. Proc., 2007 in print.
11. G.N. Morscher, “Stress-Dependent Matrix Cracking in 2D Woven SiC-fiber Reinforced Melt-Infiltrated SiC Matrix Composites”, *Comp. Sci. Tech.*, 64 pp. 1311-1319 (2004)
12. S. Kalluri, A.M. Calomino, and D. N. Brewer, “Comparison of Elevated Temperature Tensile Properties and Fatigue Behavior of Two Variants of a Woven SiC/SiC Composite,” 26 [2] Ceram. Eng. Sci. Proc, 303-310 (2005)
13. M. Steen and J.L. Valles, ASTM STP 1309, M.G. Jenkins et al., Eds. American Society for Testing and Materials, West Conshohocken, PA, 1997, pp. 49-65
14. G.N. Morscher, J. Hurst, and D. Brewer, “Intermediate-Temperature Stress Rupture of a Woven Hi-Nicalon, BN-Interphase, SiC-Matrix Composite in Air,” *J. Am. Ceram. Soc*., **83** [6] 1441-49 (2000)
15. G.N. Morscher and J.D. Cawley, “Intermediate Temperature Strength Degradation in SiC/SiC Composites,” *J. European Ceram. Soc.*, **22** 2777-2787 (2002)
16. G.N. Morscher, J.Z. Gyekenyesi, and A.L. Gyekenyesi, “Mechanical Behavior of Notched SiC/SiC Composites,” ASME International Gas Turbine and Aeroengine Congress, June 4-7, 2001, No. 2001-GT-461
17. R.T. Bhatt, G.N. Morscher, and K.N. Lee, “Influence of EBC Coating on Tensile Properties of MI SiC/SiC Composites,” Proceedings to PACRIM (2006)

18. H.M. Yun and J.A. DiCarlo, “Time/temperature dependent tensile strength of SiC and Al2O3-based fibers”, in Ceramic Transactions, Vol. 74, Advances in Ceramic-Matrix Composites III. Eds. N. P. Bansal and J.P. Singh. American Ceramic Society, Westerville OH, 1996, pp. 17-26.
19. R.T. Bhatt, T.R. McCue, and J.A.DiCarlo, “Thermal Stability of Melt Infiltrated SiC/SiC Composites,” Ceram. Eng. Sci. Proc., 24 [4] 295-300 (2003)
20. H.M Yun, D. Wheeler, Y. Chen, and J.A. DiCarlo, “Thermo-Mechanical Propterites of Super Sylramic SiC Fibers”, *Ceram. Eng. Sci. Proc.*, 26 [2] 59-66 (2005)

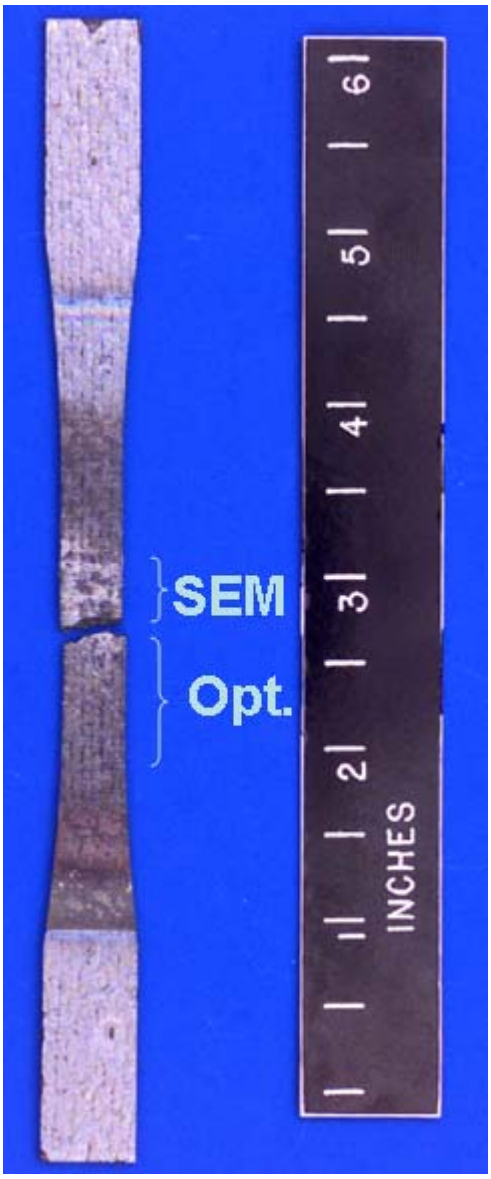

Figure 1: Typical failed specimen after creep or fatigue.

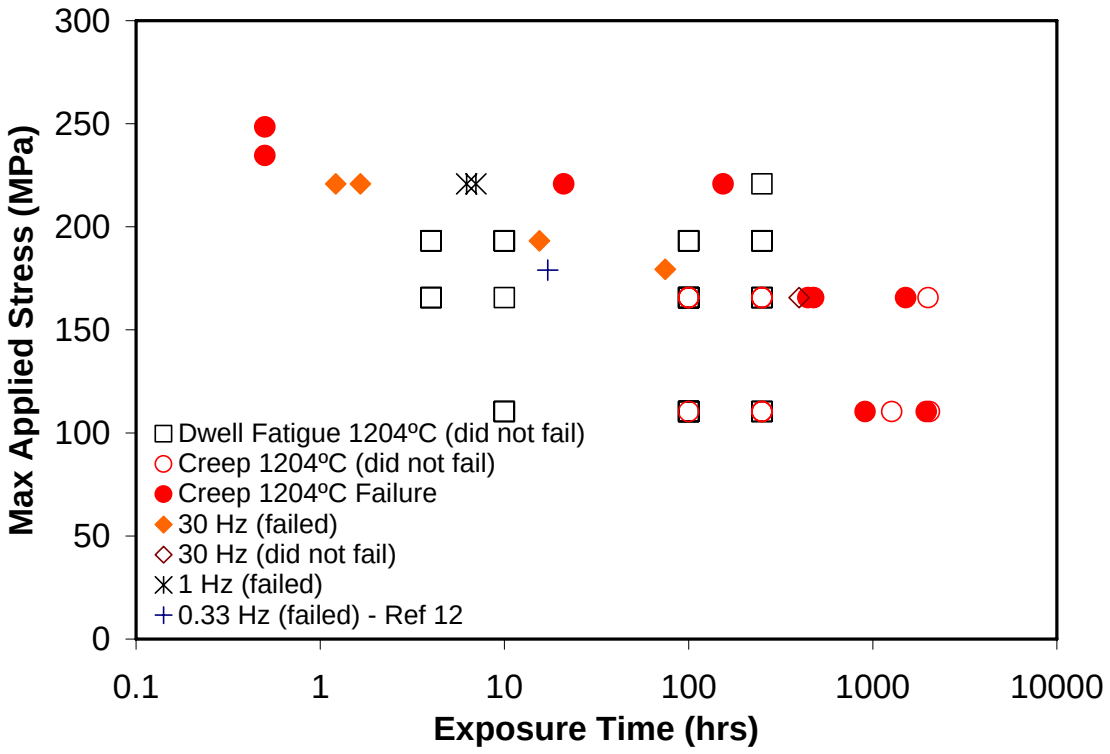

Figure 2: Creep and fatigue data versus time for the different elevated temperature tests.

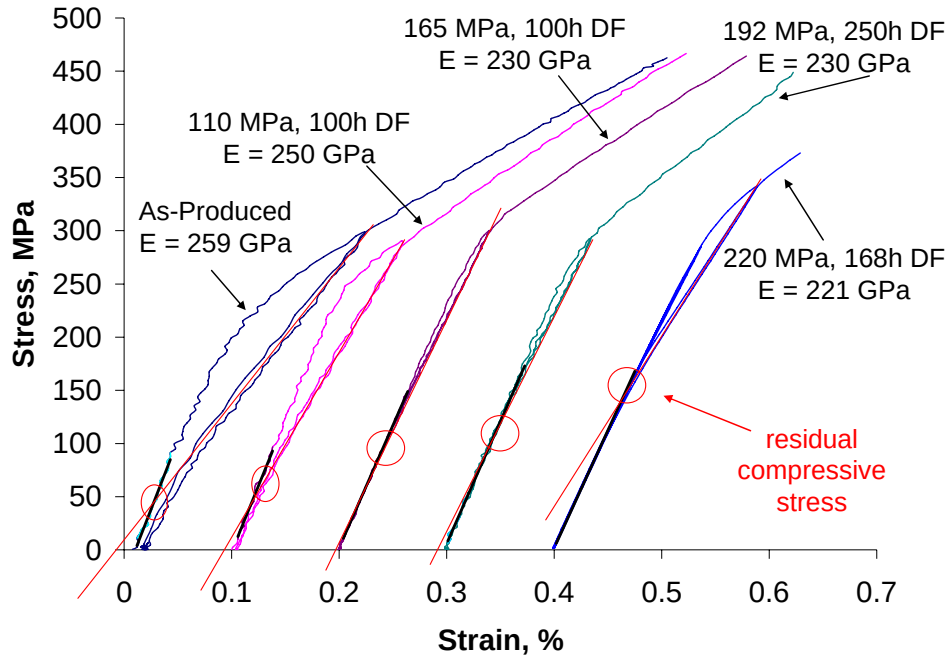

(a)

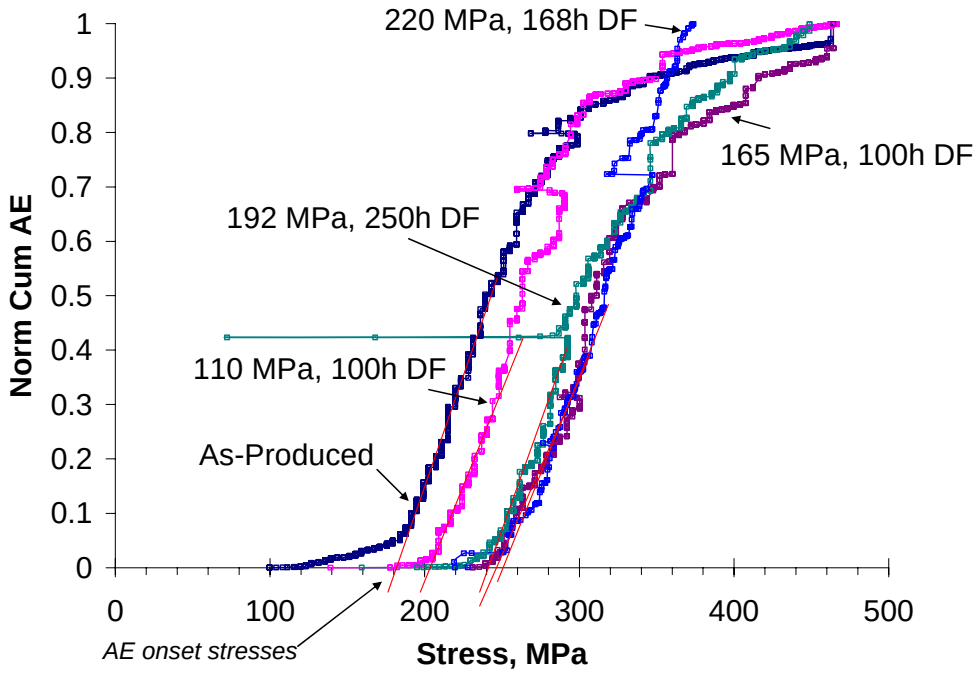

(b)

Figure 3: Room temperature stress strain behavior (a) and AE behavior (b) for an as-produced and two after-creep specimens. Note that the stress-strain curves in (a) are offset for clarity.

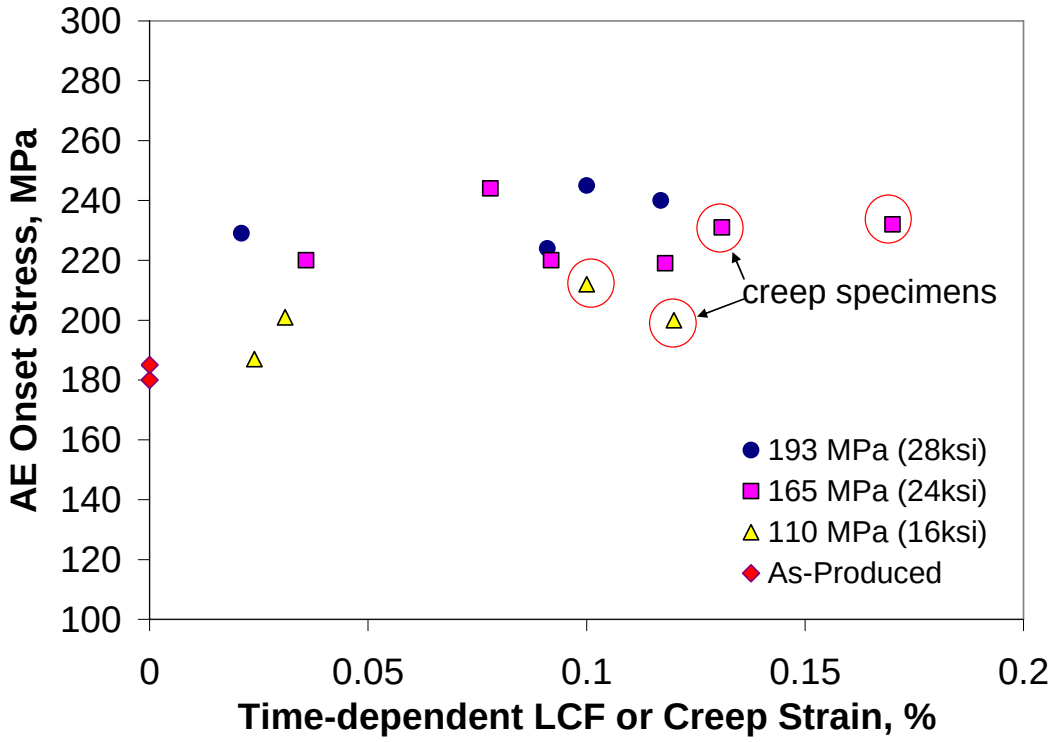

Figure 4: Room temperature AE onset stress vs time dependent strain for DF and creep (where noted) tests.

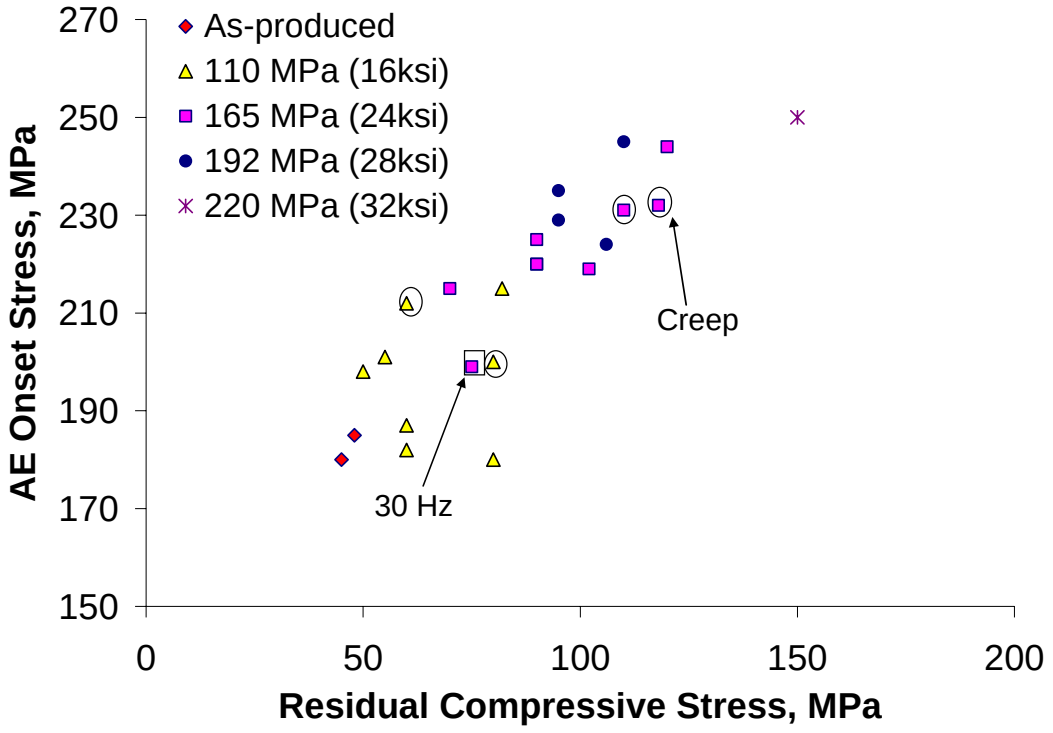

Figure 5: Matrix cracking stress as determined from AE versus the residual compressive stress in the matrix. Most of the data is for DF tests except where noted.

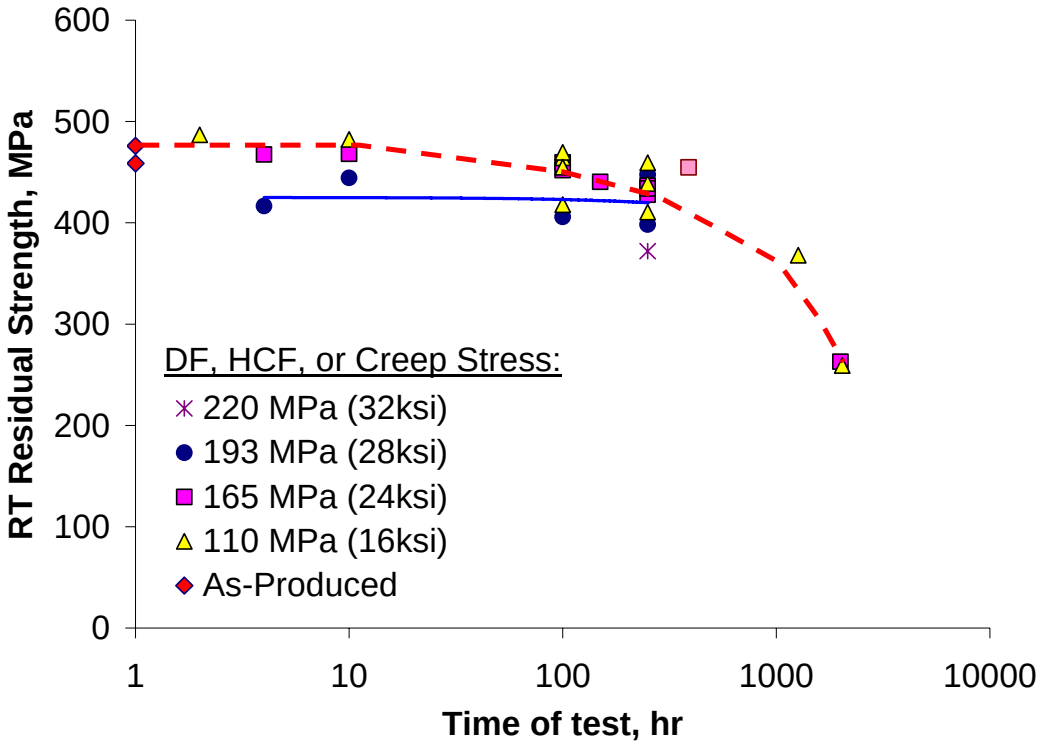

Figure 6: Ultimate strength at room temperature for as-produced and after creep or fatigue.

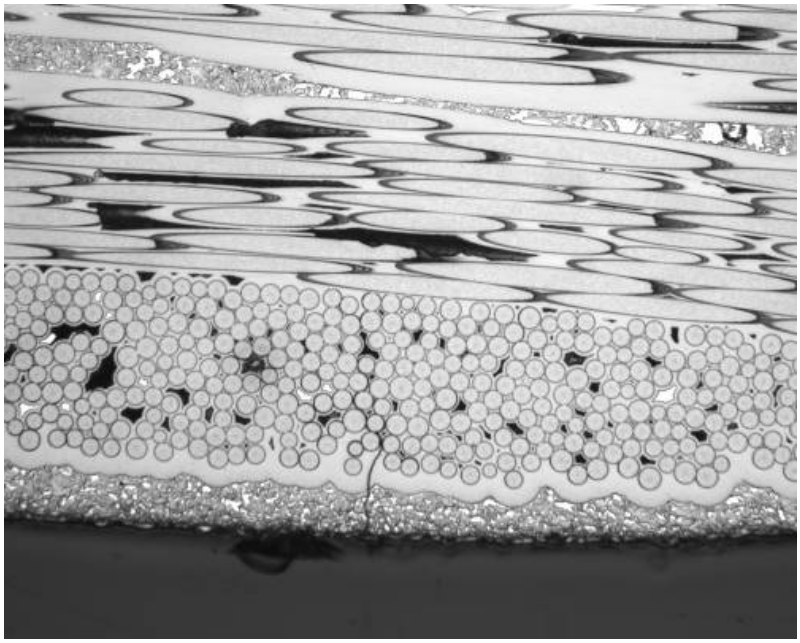

(a)

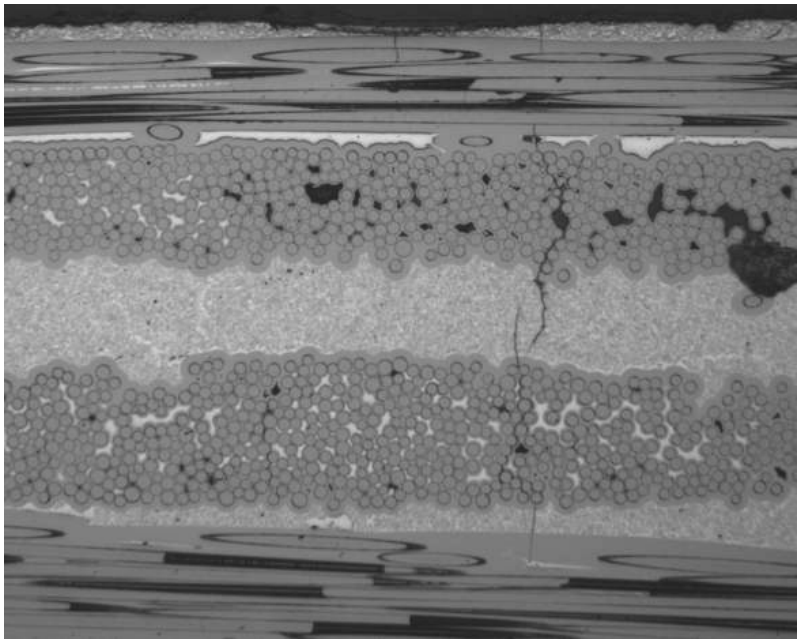

(b)

Figure 7: Typical creep-formed cracks: (a) surface 90^{o} minicomposite (110 MPa, 2036 hours, did not fail in rupture) and (b) inner back-to-back 90^{o} minicomposite cracks which extended to the surface through a 0^{o} minicomposite (165 MPa; 1508 hr creep rupture).

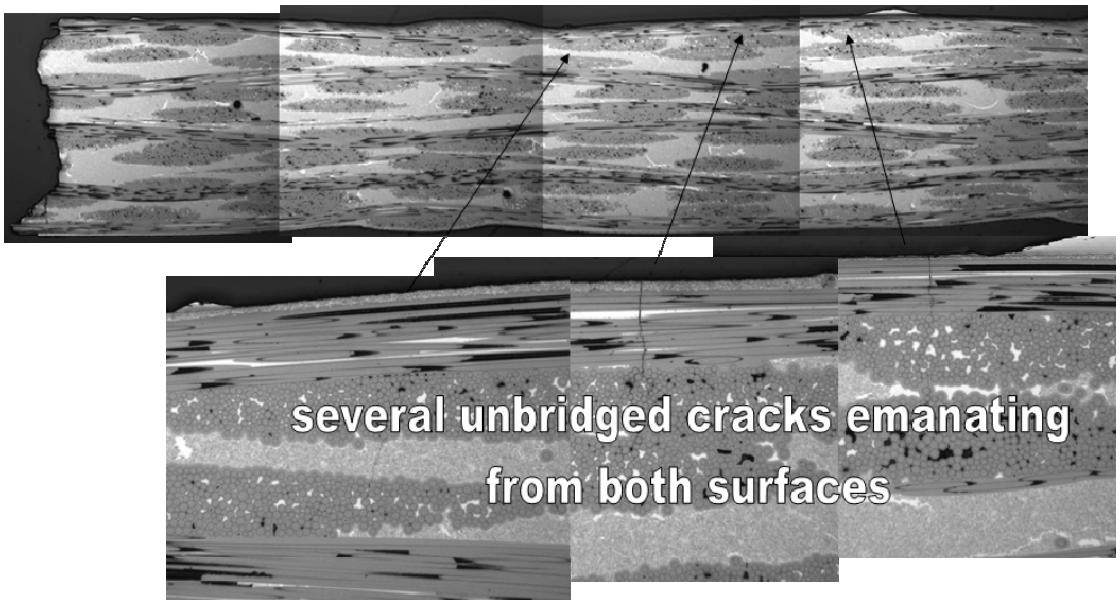

Figure 8: Matrix cracks that extend at least two plies from the surface and in some cases have fractured fibers in the matrix crack wake. This specimen had undergone 220 MPa 30 Hz fatigue and lasted approximately 1.2 hours at 1200C.

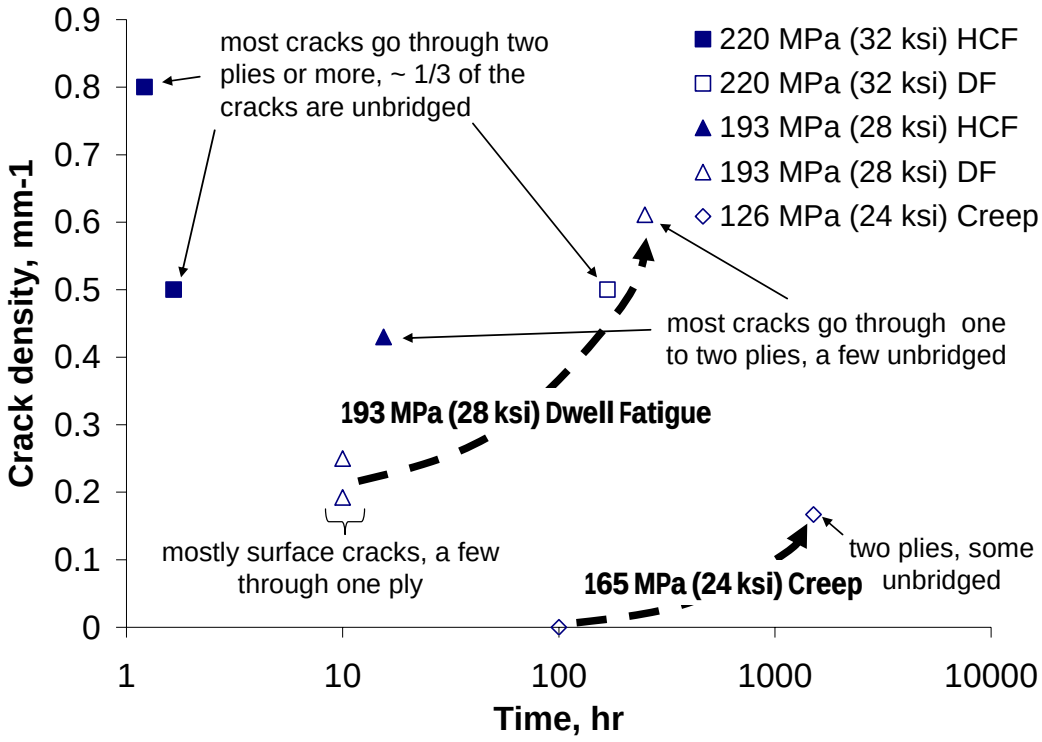

Figure 9: Crack density along the length of the specimen for different stress, time, and loading conditions.

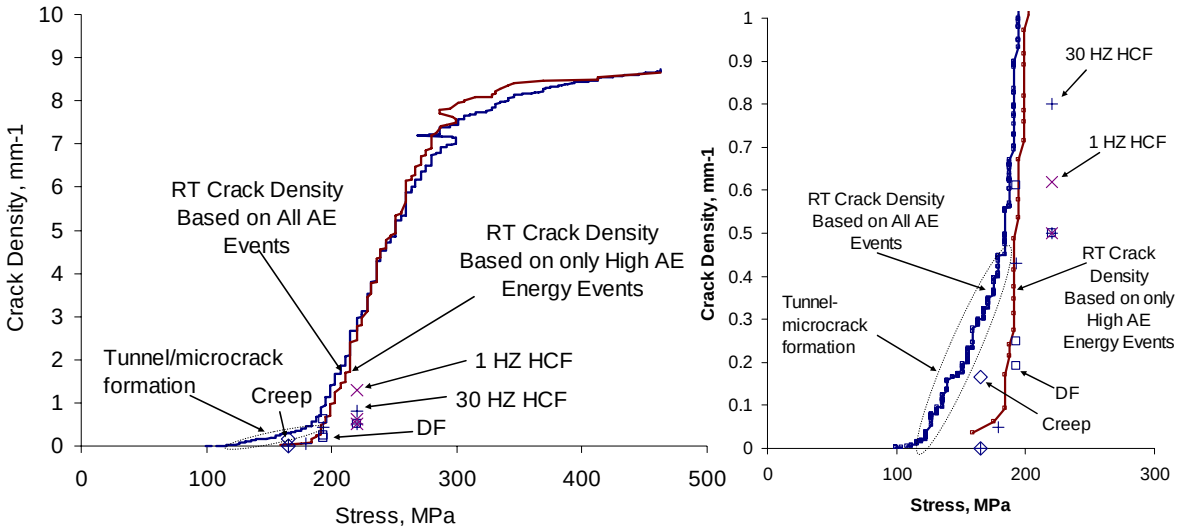

Figure 10: Matrix crack density versus stress for cracks that propagate at least 1 ply.

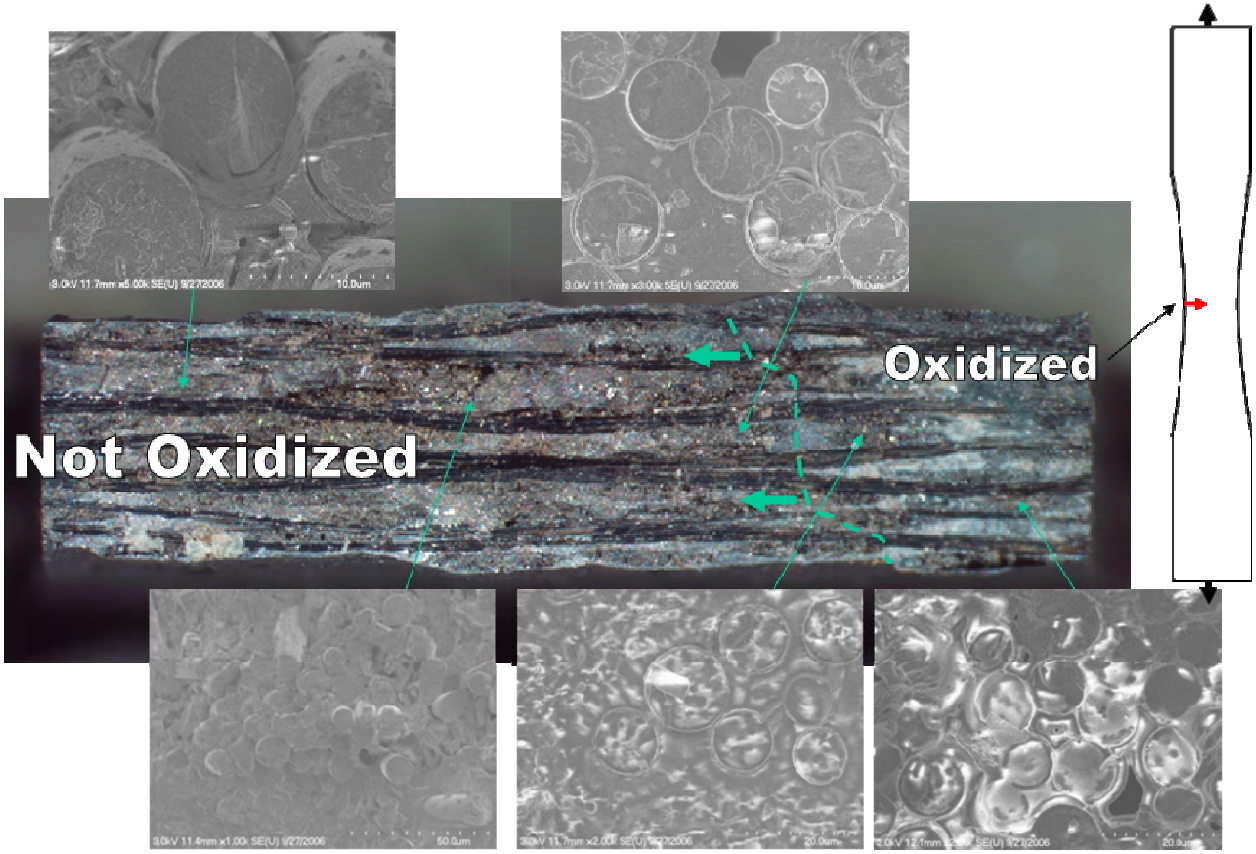

Figure 11: Typical unbridged edge-crack growth in specimen tested at 30 hz fatigue, 179 MPa for 8.1×10^6 cycles (~ 75 hrs).

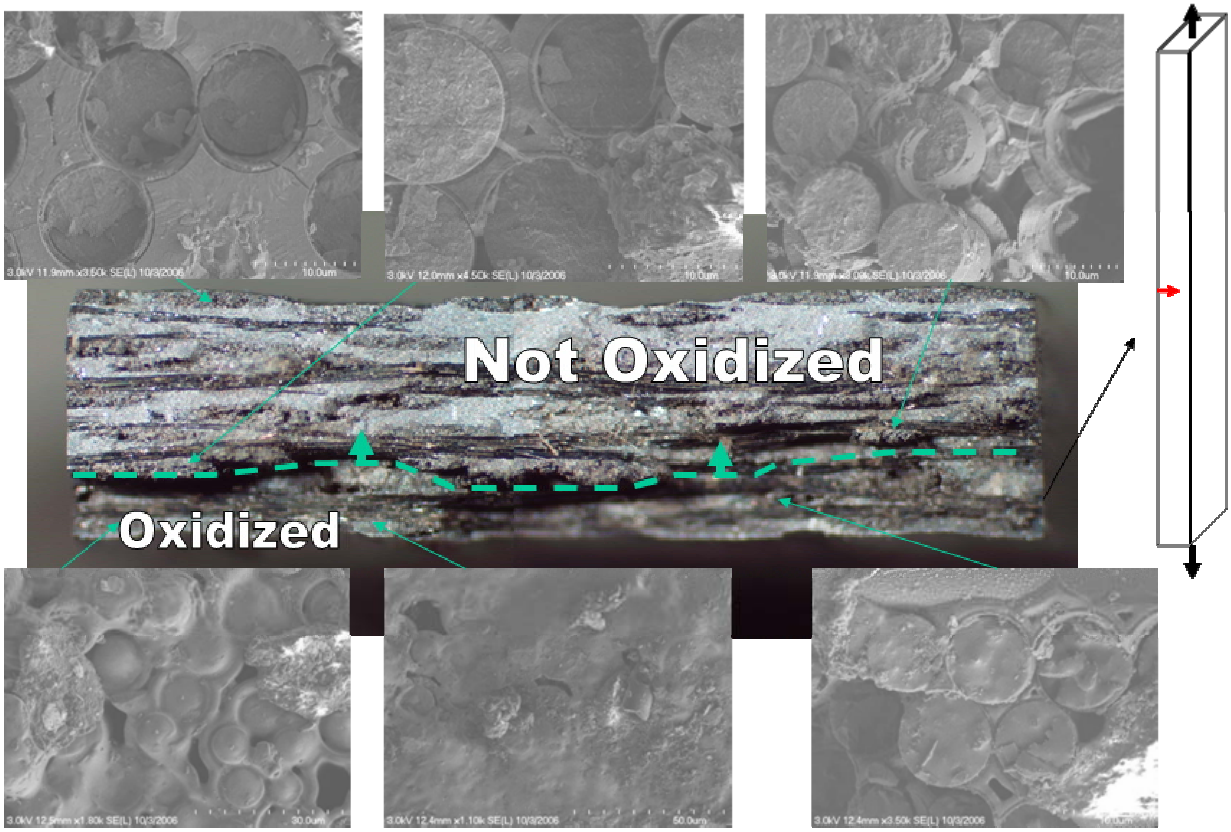

Figure 12: Less typical unbridged face-crack growth in specimen tested at 30 hz fatigue, 220 MPa for 178,493 cycles (~ 1.6 hrs).

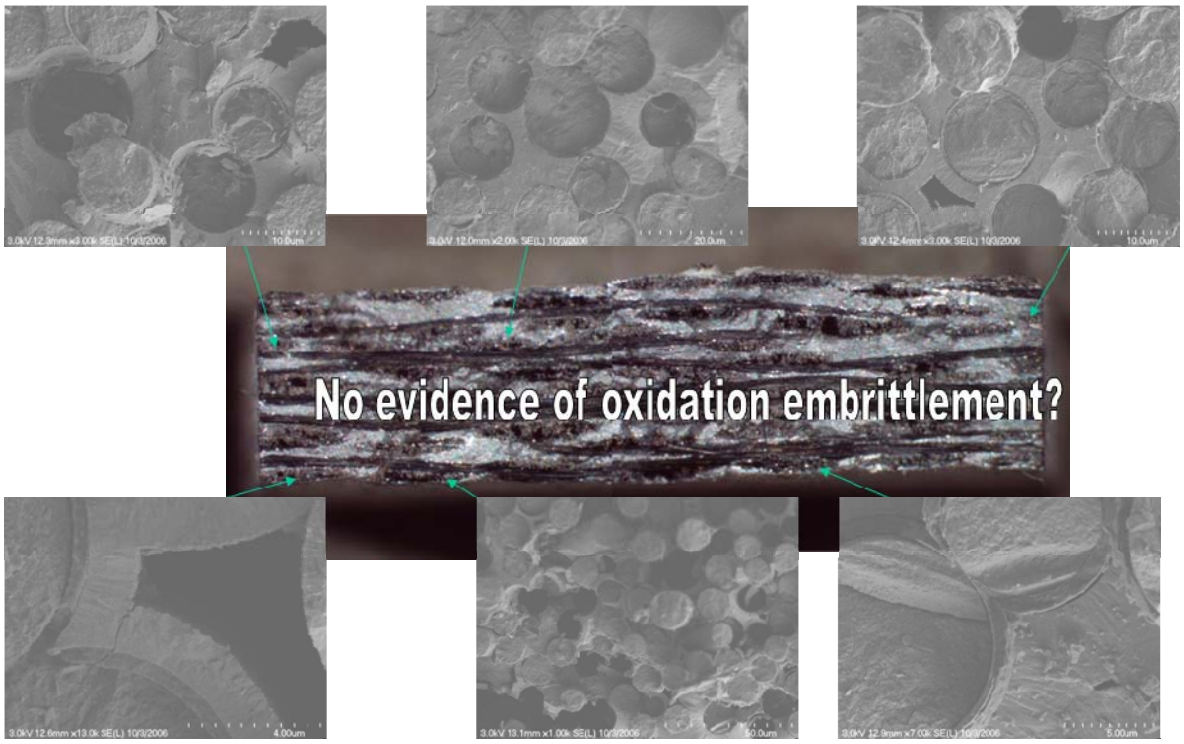

Figure 13: Fracture surface of 1300-01-006-p02, 110 MPa creep for 2036 hours followed by room temperature residual strength test, showing no oxidation at the fracture surface. The higher magnification images show no oxidation which is best seen by the presence of the BN layer around the fibers and no oxidation of SiC matrix.

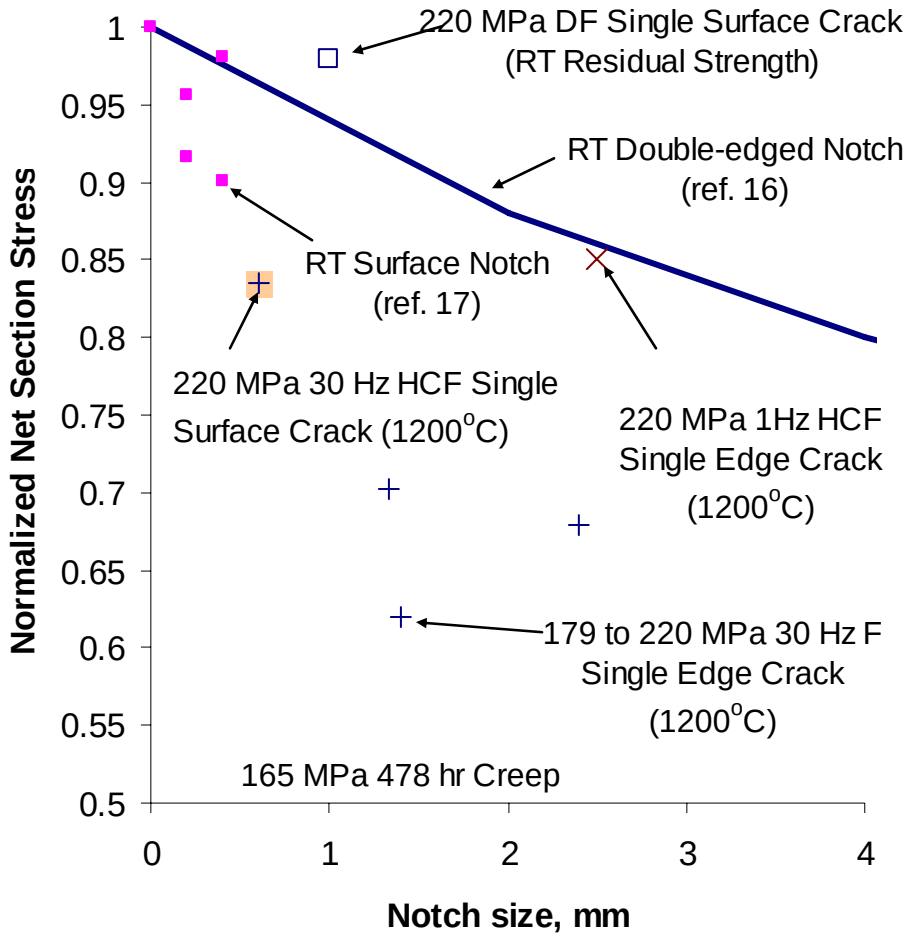

Figure 14: Normalized net section stress versus the notch or unbridged crack size.

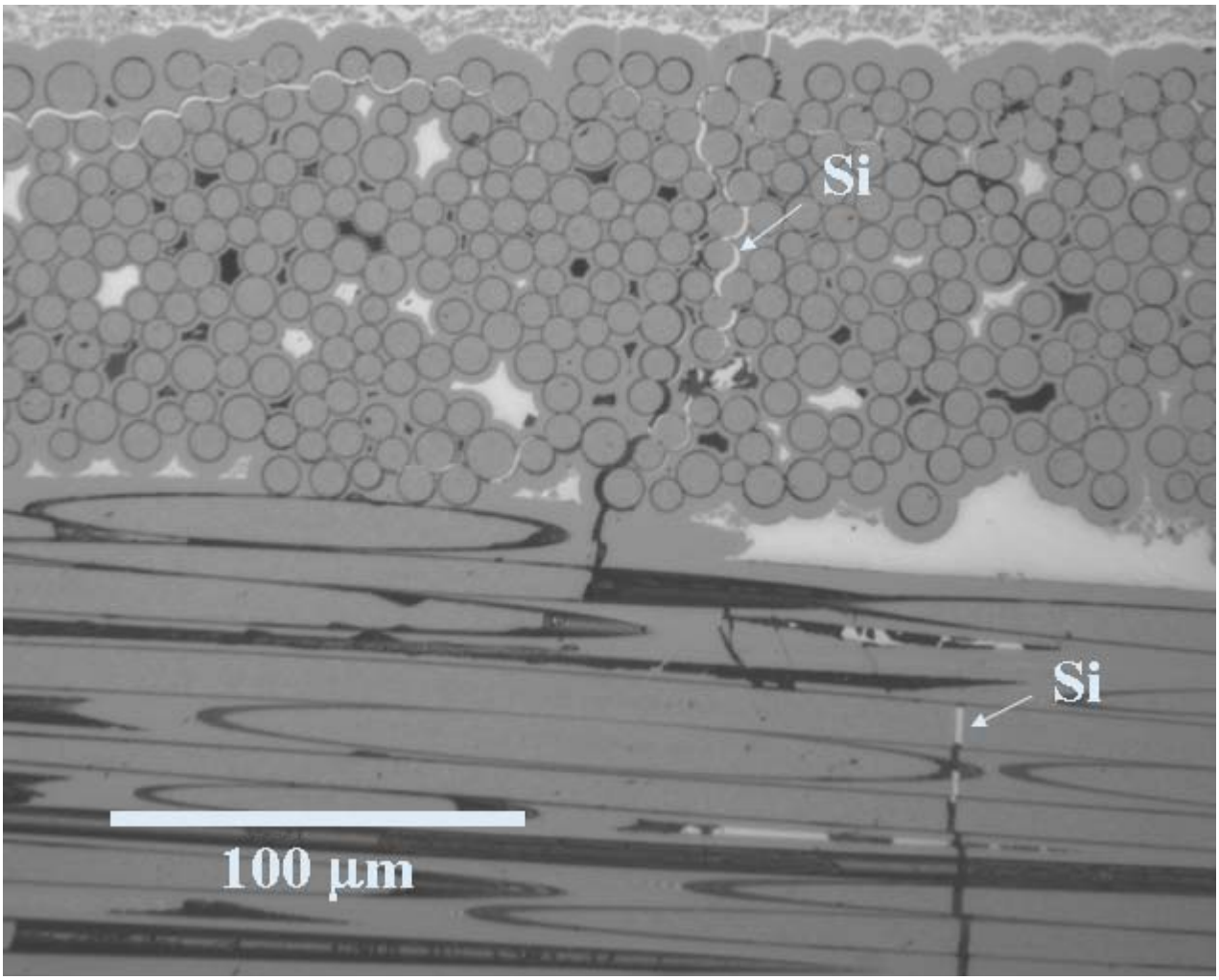

Figure 15: Micrograph of 165 MPa creep specimen that failed after 1500 hours that shows the presence of some free Si in the 90^{o} and 0^{o} minicomposite portions of an unbridged crack well away from the fracture surface.